Journal of Cardiology 64 (2014) 401–408

Contents lists available at ScienceDirect

Journal of Cardiology

journal homepage: www.elsevier.com/locate/jjcc

Original article

Non-uniform distribution of the contraction/extension (C–E) in the left ventricular myocardium related to the myocardial function

Motonao Tanaka (MD, PhD, FJCC)[a,*], Tsuguya Sakamoto (MD, PhD, FJCC)[b], Yoshiaki Katahira (MD, PhD, FJCC)[a], Haruna Tabuchi (MD)[a], Hiroyuki Nakajima (RMS)[a], Takafumi Kurokawa (RMS)[a], Hiroshi Kanai (PhD)[c], Hideyuki Hasegawa (PhD)[c], Shigeo Ohtsuki (PhD)[d]

[a] *Cardiovascular Center, Tohoku Pharmaceutical University Hospital, Sendai, Japan*
[b] *Hanzomon Hospital, Tokyo, Japan*
[c] *Department of Electrical Engineering, Tohoku University, Sendai, Japan*
[d] *Institute of Medical Ultrasound Technology, Yokohama, Japan*

ARTICLE INFO

Article history:
Received 2 December 2013
Received in revised form 5 February 2014
Accepted 18 February 2014
Available online 16 May 2014

Keywords:
Contraction/extension property
Axial strain rate
Phase difference tracking method
Non-uniformity of the C–E
Myocardial function

ABSTRACT

Objective: We attempted to disclose the microscopic characteristics of the non-uniform distribution of the contraction and extension (C–E) of the left ventricular (LV) myocardium using a new methodology (echo-dynamography).
Methods: The distributions of the "axial strain rate" (aSR) and the intra-mural velocity in the local areas of the free wall including the posterior wall (PW) and interventricular septum (IVS) were microscopically obtained using echo-dynamography with a high accuracy of 821 μm in the spatial resolution. The results were shown by the color M-mode echocardiogram or curvilinear graph. Subjects were 10 presumably normal volunteers.
Results:

(1) Both the C–E in the pulsating LV wall showed non-uniformity spatially and time-sequentially.
(2) The C–E property was better evaluated by the aSR distribution method rather than the intra-mural velocity distribution method.
(3) Two types of non-uniformity of the aSR distribution were observed: i.e. (i) the difference of its (+)SR (contraction: C) or (−)SR (extension: E) was solely the "magnitude"; (ii) the coexistence of both the (+)SR and (−)SR at the same time.
(4) The aSR distribution during systole was either "spotted," or "multi-layered," or "toned" distribution, whereas "stratified," "toned," or "alternating" distributions were observed during diastole.
(5) The aSR distribution in the longitudinal section plane was varied in the individual areas of the wall even during the same timing.
(6) To the mechanical function of the LV, there was a different behavior between the IVS and PW.

Conclusions: The aSR and its distribution were the major determinants of the C–E property of the LV myocardium. Spatial as well as time-sequential uniformity of either contraction or extension did not exist. The myocardial function changed depending on the assemblage of the aSR distribution, and by the synergistic effect of (+)SR and (−)SR, the non-uniformity itself potentially served to hold the smooth LV mechanical function.

Introduction

The mechanical pump function of the left ventricle (LV) is performed by the sacciform structure with thick walls. It is constituted from the following 4 steps of the contraction and extension (C–E) property: i.e. (1) a cellular step including sarcomere; (2) a

* Corresponding author at: Cardiovascular Center, Tohoku Pharmaceutical University Hospital, Fukumuro 1-12-1, Miyagino-ku, Sendai 983-0005, Japan, Tel.: +81 022 719 5161; fax: +81 022 719 5166.
E-mail addresses: m.tanaka@jata-miyagi.org, shin@jcc.gr.jp (M. Tanaka).

http://dx.doi.org/10.1016/j.jjcc.2014.02.024
0914-5087/

multi-cellular step; (3) a ventricular wall step (deformability); and finally (4) the step of the intra-ventricular flow structure caused by the deformation of the LV. In this respect, it has been said that the non-uniformity at each step leads to the uniformity of function at the next step [1,2]. However, the actual feature of the non-uniformity of the C–E distribution in the myocardium has been obscure until now.

In this study, we attempted to disclose the actual feature of this non-uniformity of the C–E distribution in each step and its clinical significance using non-invasive echo-dynamography. This method was used because of the difficulty of *in situ* study using conventional methodology [1–8].

Subjects and methods

Subjects

Ten presumably normal volunteers aged 30–50 (39.6 ± 10.4) years who gave informed consent were investigated.

Methods

Measurement of the axial strain rate distribution of the myocardium

In the 2D echocardiography, as described previously [9–11], the LV "longitudinal" section plane was used to minimize acoustical measurement error [9,10]. Perpendicular to this plane was the short-axis plane. As shown in Fig. 1 top, the range of the angle of 30° out of 90° was scanned at a high speed of 630–700 frame/s, transiently switching 5 beam directions evenly from the base to the apex (1–5: sparse scan). The echo signals from the wall for about 2–6 s were recorded in the memory and processed off-line by using our software [12–16].

The axial strain rate (aSR) in the local myocardial tissue of 821 μm thickness was obtained by the bottom equation (Fig. 1) using "the phase difference tracking method" [13,14].

The serial aSR distribution was obtained by shifting the measuring point of aSR at every 200 μm from the endocardium (End) to the epicardium (Epi) (the distance is about 10 mm). The minimum range of changes in the thickness accuracy was about 2 μm. The time serial aSR distribution is displayed in the color-coded M-mode images (Figs. 2 and 3). The magnitude of the aSR is shown by the color bar. The increment of the (+)aSR (contraction) is indicated by the cold color (dark to light blue tone) and that of the (−)aSR (extension), by the warm color (red to yellow tone). In between, the black zone (B in Figs. 2 and 3) indicates the relaxation shown near zero aSR.

Measurement of the contraction and extension velocity distribution

To verify the sensitivity and/or accuracy of the aSR measurement compared with that of the previous conventional methodology [13,14], the intramural velocity at many points in every 0.2 mm distance on 5 ultrasonic beams was measured at the same time. These speed data were overlapped for display in curvilinear graphs (Fig. 4). The thick velocity curves indicated that the velocities at every measuring point were different and non-uniform, and the thin curves indicated muscle fiber movement with the same velocity. Plus (+) or minus (−) signal was used for the advancing or receding movement.

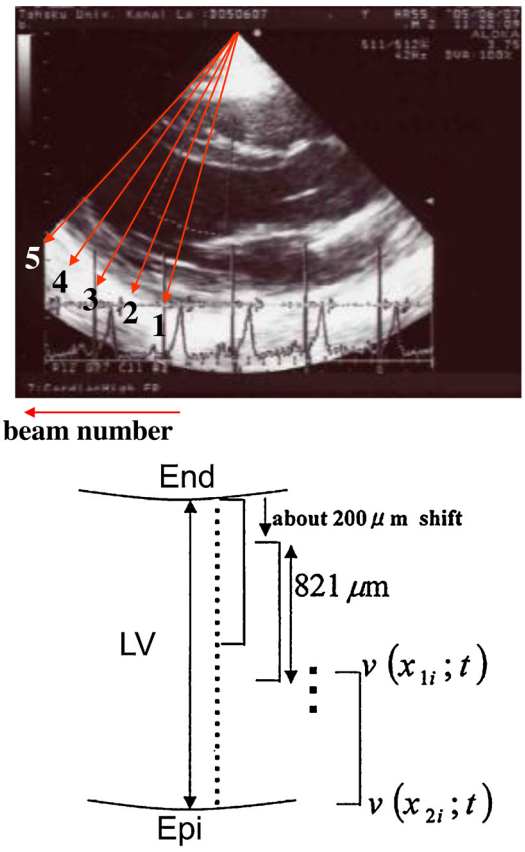

Fig. 1. Measuring process of the high resolution axial strain rate (aSR) in the myocardium by the phase difference tracking method. Upper figure: After confirmation of the heart structure in the longitudinal section plane, 5 beam directions were decided. Middle figure: In each beam direction, the measuring range is decided, e.g. from endocardium (End) to epicardium (Epi) and then, the measuring width (821 μm) was set. The velocity data [$v(x_{1i};\ t)$, $v(x_{2i};\ t)$] at two terminal points of the measuring width were calculated under the assumptive intramural velocity of 1600 m/s [16] and using difference in the distance between two points [$x_{2i}(t) - x_{1i}(t)$]. The aSR was obtained by the equation [$S_i(t)$] at the bottom. When shifting the measuring width at every 200 μm from End to Epi, the aSR distribution in the myocardium along the beam direction was obtained. LV, left ventricular wall; End, endocardium; Epi, epicardium.

Results

The results obtained were similar in all 10 subjects examined. A minor difference was seen in the heart rate among the subjects, but the general tendency was unequivocal.

The C-R/E property evaluated by the aSR distribution

Along the short-axis direction, the areas of (+) and (−)SR usually coexisted and uniform behavior was not observed. The following two types of aSR distribution were observed (Figs. 2 and 3).

(1) The black area (B in the figures, aSR ≈ 0; relaxation area) at the boundary between (+) and (−)SR;
(2) No black area between (+) and (−)SR.

In addition, two types of non-uniform distribution were observed.

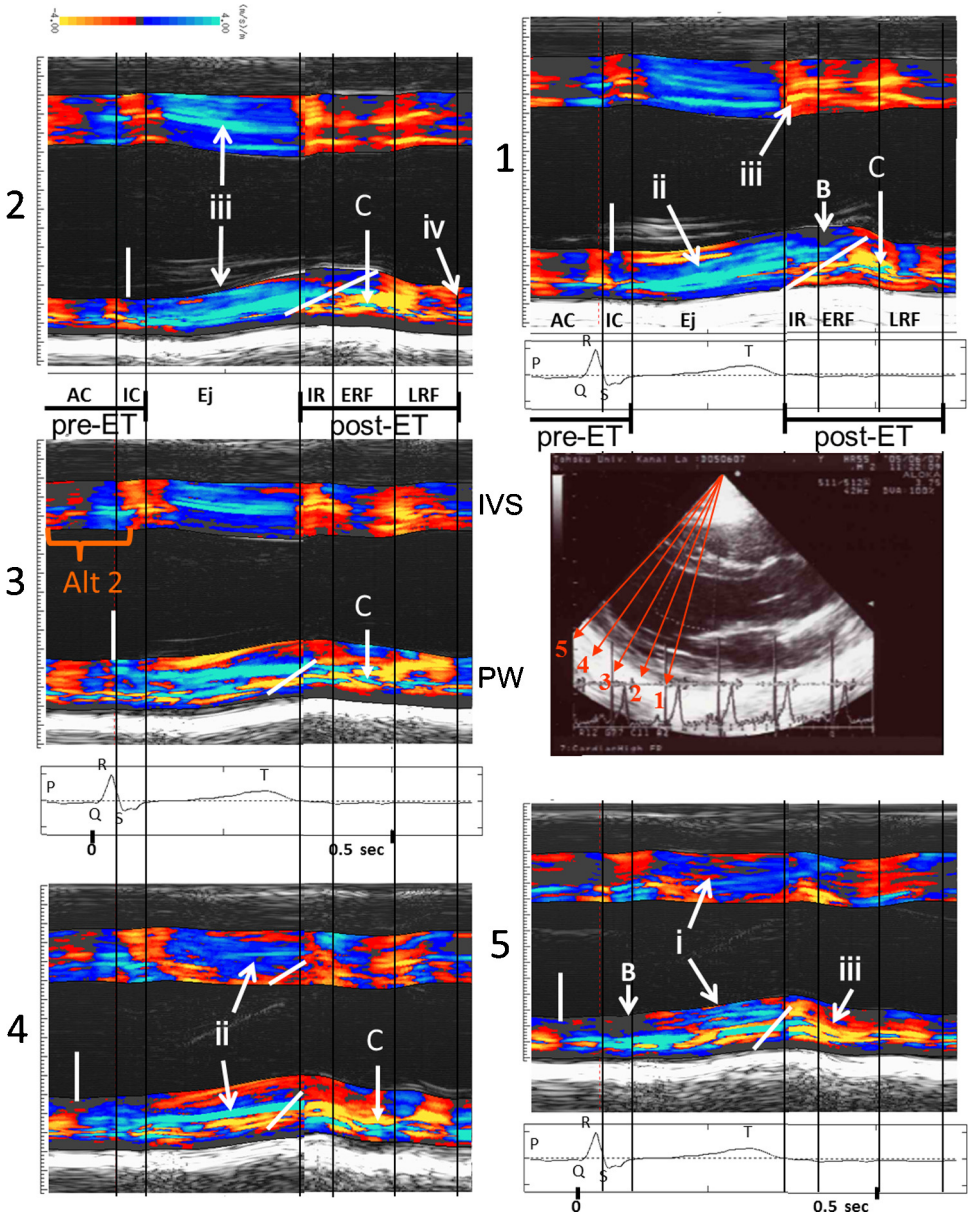

Fig. 2. M-mode images of the axial strain rate (aSR) distribution in the short-axis direction of the interventricular septum (IVS) and posterior wall (PW) measured on the longitudinal section plane during systolic to early diastolic phase. These results were obtained in the beam directions 1–5. The cold color area shows an increment of the strain rate [(+)SR; contracting] and the warm color area decrement [(−)SR; extending]. The black area (B, SR ≈ 0) shows relaxing or diastasis. The color bar demonstrates the grade of the strain rate. IC, isovolumetric contraction; Ej, ejection; IR, isovolumetric relaxation; ERF, early stage rapid filling; LRF, late stage rapid filling; SF, slow filling; AC, atrial contraction; pre-ET, pre-ejection transitional phase; post-ET, post-ejection transitional phase; white narrow oblique lines, beginning of the PW extension; white narrow vertical lines, beginning of the PW contraction; C, contracting muscle component (superficial oblique muscle); i, Spotted D; ii, multi-layered D; iii, Toned D; iv, stratified D; Alt 1, Alternating D1; Alt 2, Alternating D2; IVS, interventricular septum; PW, posterior wall; P,Q,R,S,T, ECG symbols.

(1) The magnitude of either the (+)SR or the (−)SR was unevenly distributed
(2) The non-uniform distribution produced by coexisting (+)SR and (−)SR during the same timing.

Non-uniformity in the spatial distribution of the aSR along the short axis

Considering pre-ejection transitional (pre-ET), ejection (Ej), post-ejection transitional (post-ET), and slow filling (SF) phases, characteristics of the spatial aSR distribution at the apical, central, and basal parts in each cardiac phase displayed 5 varieties (Fig. 5 and Fig. 6).

Spotted distribution. Non-uniform distribution caused by dispersing the narrow and strong (−)SR as a spotted pattern in the basic distribution of the (+)SR. Therefore, no black area was present. This distribution was frequently observed during the Ej phase at the apical part of the free wall (PW) and inter-ventricular septum (IVS). The (−)SR spot usually increased in the early ejection phase but decreased in the late ejection phase (Fig. 5-i-1). In the rapid filling (RF) phase, the (+) and (−) were reversed (Fig. 5-i-2).

Multi-layered distribution. Non-uniformity was displayed by 2 or 3 layers, viz. (−)SR appeared in the endocardial side and (+)SR in the epicardial side (Fig. 5-ii-1). Otherwise, (+)SR in the middle layer was sandwiched by the endocardial and epicardial (−)SR (Fig. 5-ii-2) during Ej. A three-layered pattern was usually observed at the apical and central parts and a two-layered pattern in the basal part

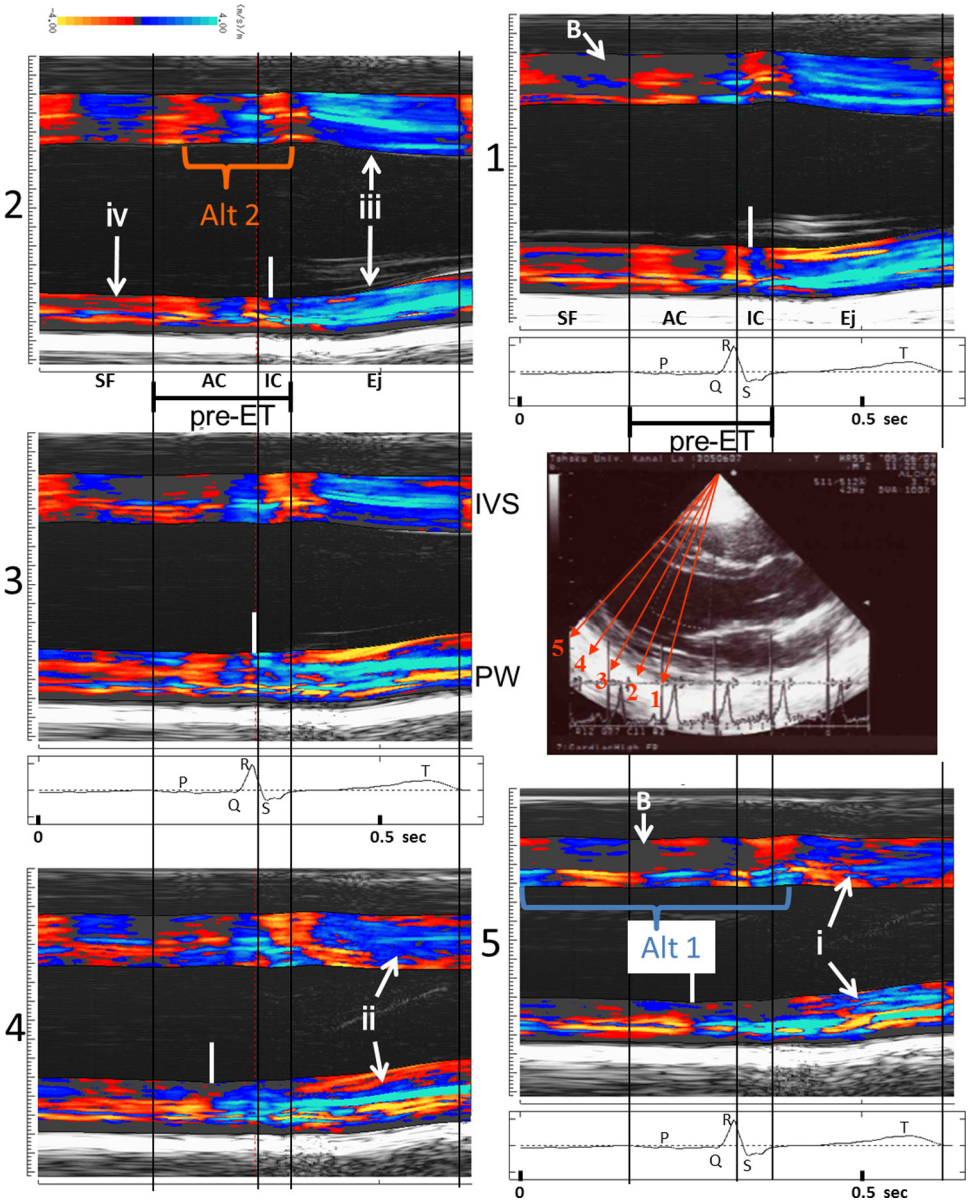

Fig. 3. M-mode images of the axial strain rate (ASR) distribution in the short-axis direction of the interventricular septum (IVS) and posterior wall (PW) during diastolic to systolic phase. These results were obtained in the beam directions 1–5 as shown in the 2D echo-cardiogram in the right middle figure. The cold color area shows an increment of the strain rate [(+)SR; contracting] and the warm color area decrement [(−)SR; extending]. The black area (B, SR ≈ 0) shows relaxing or diastasis. The color bar demonstrates the grade of the strain rate. Abbreviation: See Fig. 2.

of PW. No black area was observed at the boundary between (+) and (−)SR.

Toned distribution. As shown in the middle left of Fig. 5, the non-uniformity was displayed by either (+)SR or (−)SR. The difference in the magnitude was displayed by the changes in the color grade. This pattern was frequently observed at the basal part of the PW and IVS during Ej (Fig. 5-iii-1) or RF (Fig. 5-iii-2). This indicated that the contraction in the Ej and the extension in the RF were propagated from the epicardial side to the endocardial side. This indicated the process of transmission of the contraction or extension within the myocardium, and thus the process of displacement of the ventricular wall. In addition, the black area (SR ≈ 0, relaxation) was frequently observed at the boundary area between (+) and (−)SR.

Stratified distribution. This type was displayed by the alternately stratified arrangement of both the narrow (+)SR and (−)SR. This was observed at the PW and IVS during the SF phase. The (−)SR component at the epicardial side was larger than that at the endocardial side in the PW (Fig. 5-iv-1,2). In the IVS, it was larger at the LV side than at the right ventricular side (Fig. 3).

The black area (aSR ≈ 0) was observed widely both in the IVS and in the endocardial side of the PW as well as at the boundary area between (+) and (−)SR in the SF phase. This indicated that the active outward extension occurred at the epicardial side, whereas the diastasis or cessation of the myocardial activity occurred widely in the endocardial side during the SF phase.

Alternating distribution. The following two types of distribution were observed.

(1) The special multi-layered distribution type (Fig. 5-v-1), in which (+)SR at the endocardial side and (−)SR at the epicardial side alternate in timing with the opposite side. This

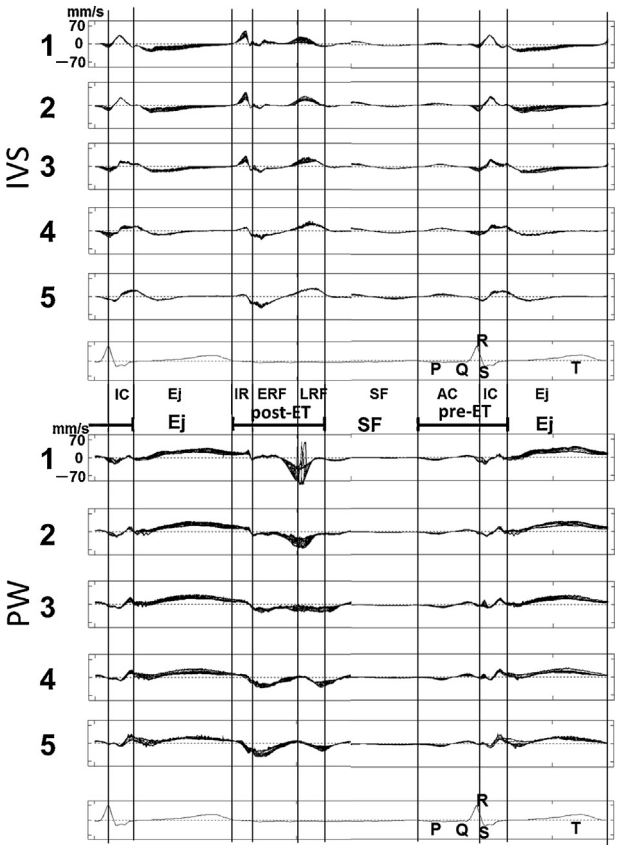

Fig. 4. Overlapped display of the curvilinear patterns of the intra-mural velocity at many points in the posterior wall (PW) and interventricular septum (IVS) obtained in the 5 beam directions at the same time. No. 1–5, beam direction. Narrow pattern means that the moving velocity of the myocardial fibers in the beam direction is almost equal. Wide pattern means that the velocity of the fibers is different within the wall (non-uniformity). IC, isovolumetric contraction; Ej, ejection; IR, isovolumetric relaxation; ERF, early stage rapid filling; LRF, late stage rapid filling; SF, slow filling; AC, atrial contraction.

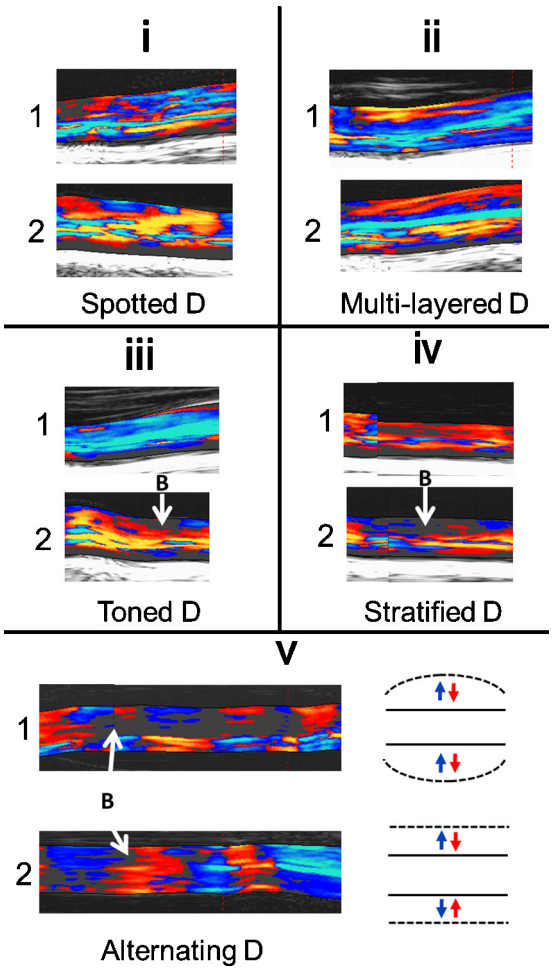

Fig. 5. Classification of the spatial distribution pattern of the axial strain rate in the wall displayed in the M-mode image. Non-uniformity of the (+) and (−)SR distribution appeared in the left ventricular wall and is classified as 5 types. The right bottom figures show schematic display of the production mechanism of type (v), viz. thickness oscillation of the wall will occur as shown by blue and red arrows. 1 and 2 are different types in the oscillation mode. B, relaxing area; blue arrows, contraction; red arrows, extension.

was observed at the apical part of the IVS during the SF to the IC phase. The black area (aSR ≈ 0) was present in the mid-layer.

(2) The special toned distribution type (Fig. 5-v-2), in which large (−)SR and (+)SR appear successively. The large SR component was observed at the basal part of both the IVS and PW during the pre-ET phase followed by the (−)SR component. The black area was observed at the boundary between the two components.

Spatial aSR distribution in the long-axis section plane

The characteristics was estimated by the aSR distribution from the apex to the base at each of the 4 cardiac phases (Figs. 2, 3 and 6).

A different type of aSR distribution appeared in the apical, central, and basal parts of the LV wall at the same cardiac phase. For example, during the Ej in the PW, the spotted distribution was shown in the apical part, the multi-layered distribution with three-layered type in the central part and the double-layered type in the basal part. During the pre-ET in the PW, when the (+)SR component was shown at the apical part, the alternating distribution 2 with large (−)SR component appeared at the basal part, but in the post-ET phase, when the large extent of (+)SR component showed at the basal part, the large (−)SR component appeared at the apical part (Fig. 6).

Estimation of the non-uniformity of the C–E property by the intra-mural velocity distribution

The curvilinear graph of the intra-mural velocity distribution in the IVS and PW during one cardiac cycle is shown in Fig. 4.

The widened (thick) velocity curve indicated that the moving velocity of the local area was not uniform. The thin curve indicated nearly equal velocity.

The apical part in the IVS moved almost uniformly through one cardiac cycle, whereas the basal part had the non-uniform velocity distribution. The velocity difference was about 20–30 mm/s throughout the pre-ET and the early rapid filling (ERF), and about 30 mm/s in the RF. Throughout the SF and the anterior half of the atrial contraction (AC), the moving velocity was almost uniform.

The velocity differences in the PW were observed in the entire wall throughout the posterior half of the AC and the late rapid filling (LRF). The difference in the velocity was about 30 mm/s in the Ej and about 65 mm/s in the RF.

However, the difference was small throughout the SF and anterior half of the AC. The difference occurred during systolic phase, but the extending velocity in the diastolic phase was nearly the same and uniform.

IVS

	Pre ET		Ej		Post ET		SF	
(1) Bas. Comp.	iii	Toned(Alt 2) (−)(+)SR	iii	Toned (+)SR	iii	Toned (−)SR	iv	Stratified (−)SR
(3) Cent. Comp.	iii	Toned(Alt 2) (−)(+)SR	ii	Multi–Layered (+)SR	iii	Toned (−)(+)SR	iv	Stratified (−)SR
(5) Ap. Comp.	ii	Multi–Layered(Alt 1) (−)(+)SR	i	Spotted (+)SR	ii	Multi–Layered(Alt 1) (−)(+)SR	ii	Multi–Layered(Alt 1) (−)(+)SR

PW

	Pre ET		Ej		Post ET		SF	
(1) Bas. Comp.	iii	Toned(Alt 2) (−)(+)SR	ii	Multi–Layered (+)SR	ii	Multi–Layered (+)SR	iv	Stratified (−)SR
(3) Cent. Comp.	iii	Toned(Alt 2) (−)(+)SR	ii	Multi–Layered (+)SR	i	Spotted (−)SR	iv	Stratified (−)SR
(5) Ap. Comp.	iii	Toned (+)SR	i	Spotted (+)SR	iii	Toned (−)SR	iv	Stratified (−)SR

Fig. 6. Classified table of the spatial distribution patterns of the aSR in the IVS and PW displayed in Figs. 2 and 3. Vertical column; (1), (3), (5), beam directions; Bas, basal part; Cent, central part; Ap, apical part; Comp., occupied component of the SR, viz. (+)SR or (−)SR; Horizontal column; cardiac phases, Pre-ET, pre-ejection transition phase; Ej, ejection phase; Post-ET, post-ejection transition phase; SF, slow filling phase; Alt 1 and 2, alternating distribution type 1 and type 2.

Correlation between the aSR distribution and the intra-mural velocity distribution

The correlation between the two was as follows:

In case of the "toned" distribution, the width of the velocity distribution was widened.
In case of the "multi-layered" distribution, it was either narrow or widened. The amount of the movement was known, but the direction and changes in thickness were not known, so the differentiation between the contraction and the extension was difficult.
In case of the "spotted distribution," the width of the velocity distribution depended on the magnitude of the aSR distribution. The above-mentioned differentiation was also difficult.
In case of the "stratified or spotted distributions [coexistence of small (−) and (+)SR]," the width of the velocity distribution was narrow and flat. Also, the same was true in the differentiation.

Discussion

Usefulness of the aSR distribution method

Brutsaert et al. [1,2] stated that the cardiac muscle function is constituted from several steps of the contraction and relaxation/extension (C–E) property. The non-uniformity was supposed to exist in the C–E property, and also, as a whole, such a non-uniformity at each small step leads to the uniformity of function at the next large step. To evaluate such a mechanism in the LV wall, it is necessary to estimate the non-uniformity of the C–E property at the muscle fiber level [5,7,8]. However, it is difficult to measure clinically the length of the muscle fiber or sarcomere. The change in the fiber length is in inverse proportion to the thickness change of the fiber or the wall [17,18]. The reason why we measure the thickness is in the fact that the thickness change is easy to measure with a great accuracy. In this regard, the non-invasive measurement of the aSR distribution seemed to be an adequate methodology.

The non-uniformity in the mechanical performance of the LV wall has been studied by many investigators utilizing ultrasonic methods [19–29]. It was thought that the velocity gradient in the myocardium [24] and the non-uniformity of the velocity [25,26], as well as the strain of the ventricle [27–29] were valuable for evaluating the myocardial function.

However, when comparing the measurement of the aSR distribution with the moving velocity distribution, it was disclosed that the latter was inadequate to evaluate the C–E property, though it was able to evaluate the movability of the myocardium. This is because the parallel existence of the contraction [(+)SR] and extension [(−)SR] during the same time makes it difficult to measure the changes in the fiber length. Therefore, the aSR distribution method seemed to be more useful in studying the C–E property of the LV wall.

Correlation between the spatial distribution of the aSR and C–E property in respect to the mechanical performance of the LV wall

The present study disclosed that contracting [(+)SR], extending [(−)SR] and relaxing (SR ≈ 0; B) areas always coexisted in the pulsating myocardium. The grade of the contraction or extension was decided by the magnitude and extent of the basal (+)SR or (−)SR components in comparison with those of the antagonistic component, which is adequately evaluated by the spatial non-uniform distribution of the aSR.

This spatial distribution pattern of the aSR was classified into 5 patterns (Figs. 5 and 6): spotted, multi-layered, toned, stratified, and alternating distribution patterns.

The "spotted," "multi-layered," and "toned" distribution patterns were observed in the systolic phase, whereas "toned," "stratified," and "alternating" distribution patterns were seen in the diastolic phase. The genesis and the plausible physiological significance of each are as follows:

The "spotted distribution" pattern was observed at the apical part during the Ej and is thought to be produced by either the pre- or afterload provided by the muscle fiber contraction in its early and mid stages.

Firstly, the contraction of the LV wall begins at the epicardial side of the apical part and propagates toward both the endocardial side and the basal part [30]. At this time, the initially contracted muscle tissue may induce the extension of the relaxed adjacent muscle tissues [31]. As a result, the adjacent muscle tissue is given the preload and shows the (−)SR. Thereafter, the muscle tissue produces larger power in the contraction stage and shows the (+)SR. Likewise, (−)SR may appear whenever this contracting muscle extends to the next adjacent muscle tissue, but, in turn, the next adjacent muscle tissue will begin to contract and (+)SR will appear, owing to the stronger contracting power. When such a phenomenon occurs successively, the larger contracting power is produced in the apical part [3] and the area of (+) or (−)SR is inscribed as a spot.

Secondly, in the multi-cellular cardiac muscle tissue, the direction and arrangements of the ventricular muscle fiber and bundle are more complicated, particularly at the apical part [8,32–34]. Whenever the intra-ventricular pressure rises during the contracting state, pressure load sensitivity in the multi-cellular cardiac muscle inevitably changes depending on the direction of the muscle fiber or muscle bundle.

The myocardial stress induced by the pressure load (afterload) may also change [35], where the high load will extend fibers despite being in the contracting state, so the (−)SR will be recorded. While at the low loading part, the fibers may be exclusively in the contracting state without extension, so (+)SR is inscribed and thus the

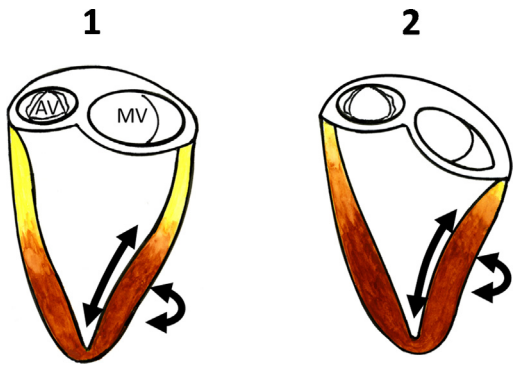

Fig. 7. Schematic representation of the extension produced in the epicardial and endocardial sides of the left ventricular wall during systole in the type ii axial strain rate (aSR) distribution. (1) Early ejection phase: The extension [(−)SR] along the circumferential direction in the epicardial side (black curved arrow) was produced by the decrement of the internal diameter with the increment of the intra-ventricular pressure and thickness (increasing the afterload). (2) Mid ejection phase: The extension [(−)SR] in the endocardial side (black long arrow) was produced in the longitudinal direction by the inward extrusion of the endocardial side of the posterior wall (PW), with the downward movement of the mitral ring and shortening of the long-axis direction in the PW during systole. AV, aortic valve; MV, mitral valve.

spotted (−)SR distribution is shown in the myocardium. In these situations, the extension of the muscle fiber occurs even under the contracting state, and the relaxing condition [black area (SR ≈ 0)] does not appear at the boundary area between (+) and (−)SR components. When the muscle tissue load increases during contracting state, large contracting power might be produced compared with that at the low load state [3,4]. The spotted distribution signifies that the apical part greatly contributes to the pressure production in the LV.

The "multi-layered distribution" was observed at the apical and central parts of the LV during the Ej. Whenever the curvature of the endocardial surface on the cross-section of the apical and central parts during contraction decreases together with increment of the thickness and intra-ventricular pressure (increment of the afterload), the circumferential stress in the muscle layer near the epicardium increases and the tension develops in the epicardial side (Fig. 7-1) [35]. Thus the (−)SR will appear near the epicardium in the circumferential direction despite being in the contracting state.

In the longitudinal section plane, as shown in Fig. 7-2, whenever the shortening of the PW in the longitudinal direction occurs during contraction together with increment of the thickness, the extrusion of the PW will occur in the internal direction together with the downward movement of the mitral valve ring. Thus, the stress (afterload) in the longitudinal direction (meridian direction) [35] may increase in the endocardial side, and the (−)SR may appear in the endocardial part. Only the middle layer was in the contracting state ((+)SR). As a result, the three-layered pattern is produced in the PW. In this situation, the extension of the muscle layers occurs during contracting state of the Ej. Therefore, the relaxing area (black area, SR ≈ 0) does not appear at the boundary area.

During contracting state, the (−)SR component may act as the afterload to the myocardium, then the contracting muscle may produce stronger power than that in the case without extension [3,4]. In the case where the "multi-layered distribution" appears only in the endocardial side, the same effects will be produced.

From these results, the apical and central parts seemed to contribute to produce the large contracting power and to act as the controller for producing and maintaining the intra-ventricular pressure.

The "toned" distribution appeared at the basal part of the LV wall in both the systolic and diastolic phases. The magnitude of the aSR showed the level of either the contraction or the extension of the myocardium. Whenever the level of the (+)SR is larger in the endocardial side, the increment of the thickness is large in this side, and thus the displacement increases toward the inner side, so the internal diameter of the LV decreases. When the level of (−)SR is larger in the epicardial side than that in the endocardial side, the latter will displace toward the outer side (dilatation) and produce an increment of the LV volume, thus the basal part acts as the controller of the flow volume in the LV. The relaxing area (SR ≈ 0) appeared at the boundary between (+) and (−)SR.

The "stratified" distribution appeared in the SF phase. In the PW, the (−)SR component near the epicardial side was usually larger than that along the endocardial side, and the (+)SR component near the epicardial side was also large. The (+)SR component acts as an extender to the relaxing area, inducing a (−)SR component. Thus the gentle contraction may induce the gentle extension in the adjacent tissue. It is considered that the gentle active expansion (dilatation) may occur toward the epicardial side during the SF. Therefore, the relaxing area (black area; SR ≈ 0) is widely observed in the IVS and the PW during SF.

Based on the observation of the "toned" and "stratified" distributions, the basal part is considered to act as the controller of the flow volume in the ventricle.

The "alternating" distribution was observed in the IVS during the RF and pre-ET phases. Considered together, these findings indicate that the thickened muscle oscillation may occur during extending state by the power of the eddy flow [36,37] as shown in the right bottom schema in Fig. 5.

Type (1) may be produced by multiple small eddies under the negative or low pressure condition [36], and type (2) by the large rotating flow occurring under the high pressure condition [11,37] during the pre-ET phase.

On the other hand, the aSR distribution in the longitudinal section plane showed a different type of distribution in each part of the apex, center, and base at the same cardiac phase. This indicated that a synergistic effect of the function is produced in the LV wall as seen in the Ej phase. The producing effect of the intra-ventricular pressure in the apical part, the maintaining effect of the increased pressure in the central part and the volume controlling effect in the basal part may all cooperate with each other, and thus an effective ejection may be accomplished.

Limitations

Several limitations need to be mentioned. First, the number of cases was rather small, precluding a statistical study. Second, the technology of "phase difference tracking method in ultrasonics" is not widely used because it was developed in our own laboratory, and is not familiar to other investigators at the present time.

Finally, we have to obtain clinical feasibility by investigating the relationship between the C–E property in the local myocardium and the deformability of the LV, and further to obtain the related pump function in cases with various pathological states. Therefore, further observation is mandatory.

Conclusions

The C–E property of the local ventricular muscle was investigated using high-resolution aSR measurement. Analysis was made on the characteristics of the C–E property in the PW and IVS, and the correlation between the non-uniformity of the SR distribution and the LV wall function was also obtained.

The C–E property was not so simple compared with the theory of the previous investigators. Our investigation showed that the non-uniformity of the contraction and extension in the LV myocardium

and its spatial distribution were the determinants of LV performance. From the standpoint of the aSR distribution, the myocardial function changed depending on the assemblage of the aSR distribution and the cooperation, each area of the LV seemed to share an individual role in maintaining pump function. The non-invasive measurement of the aSR is thought to be foresighted and useful to investigate the myocardial function as a whole.

References

[1] Brutsaert DL, Sys SU. Relaxation and diastole of the heart. Physiol Rev 1989;69:1228–315.
[2] Brutsaert DL, DeClerk NM, Goethals MA, Housmans PR. Relaxation of ventricular cardiac muscle. J Physiol 1978;283:469–80.
[3] Ishida N, Takishima T. Dynamics of the myocardium. Cardiodynamics and its clinical application. 2nd ed. Tokyo: Bunkodo Co.; 1992. p. 1–63.
[4] Braunwald E, Sonnenblick EH, Ross Jr J. Contraction of the normal heart. In: Braunwald E, editor. Heart disease, vol. I, 2nd ed. Philadelphia: WB Saunders Co.; 1984. p. 409–46.
[5] Matsuda K, editor. Japanese handbook of physiology, vol. III. Physiology of circulation. Tokyo: Igakushoin Ltd.; 1969. p. 70–147.
[6] Barnett VA. Cardiac myocytes. In: Iaizzo PA, editor. Handbook of cardiac anatomy, physiology, and devices, Part III. New Jersey: Humana Press Inc.; 2005. p. 113–21.
[7] Sonnenblick EH, Ross Jr J, Covell JW, Spotnitz HM, Spiro D. The ultrastructure of the heart in systole and diastole: changes in sarcomer length. Circ Res 1967;21:423–31.
[8] Rushmer RF. Functional anatomy and control of the heart. Cardiovascular dynamics. 4th ed. Philadelphia: WB Saunders Co.; 1970. p. 76–131.
[9] Tanaka M. Ultrasonic diagnosis of the heart. 1st ed. Tokyo: Medic. Elecro-Times Ltd.; 1978.
[10] Tanaka M. Historical perspective of the development of echo-cardiography and medical ultrasound. In: Schneider SC, Levy M, McAvoy BR, editors. Proc IEEE Ultrasonic Symp, vol. 2. New York: IEEE Inc; 1988. p. 1517–24.
[11] Tanaka M, Sakamoto T, Sugawara S, Nakajima H, Katahira Y, Ohtsuki S, Kanai H. Blood flow structure and dynamics, and ejection mechanism in the left ventricle: analysis using echo-dynamography. J Cardiol 2008;52:86–101.
[12] Tanaka M, Kanai H, Sato M, Chubachi N. Moving velocity measurement in the local myocardial tissue by the phase difference tracking method. J Cardiol 1996;28(Suppl. I):163.
[13] Kanai H, Hasegawa H, Chubachi N, Koiwa Y, Tanaka M. Noninvasive evaluation of local myocardial thickening and its color-coded imaging. IEEE Trans Ultrson Feroelect Freq Contr 1997;44:752–68.
[14] Kanai H, Hasegawa H, Chubachi N, Koiwa Y, Tanaka M. Non-invasive evaluation of spatial distribution of local instantaneous strain energy in heart wall. In: Lees S, Ferrari LA, editors. Acoustic imaging, vol. 23. New York: Plenum Press; 1997. p. 187–92.
[15] Yoshiara H, Hasegawa H, Kanai H, Tanaka M. Ultrasonic imaging of propagation of contraction and relaxation in heart walls at high temporal resolution. Jpn J Appl Phys 2007;46:4889–96.
[16] Tanaka M, Dunn F. Acoustic properties of the fibrous tissue in myocardium and detectability of the fibrous tissue by echo method. In: Dunn F, Tanaka M, Ohtsuki S, Saijo Y, editors. Ultrasonic tissue characterization. Tokyo: Springer-Verlag; 1996. p. 231–43.
[17] Spotnitz HM, Sonnenblick EH, Spiro D. Relation of ultrastructure to function in the intact heart: sarcomere structure relative to pressure volume curves of intact left ventricles of dog and cat. Circ Res 1966;18:49–66.
[18] Laks MM, Nisenson MJ, Swan HJC. Myocardial cell and sarcomere length in the normal dog heart. Circ Res 1967;21:671–98.
[19] Bogaert J, Rademakers FE. Regional non-uniformity of normal adult human left ventricle. Am J Physiol Heart Circ Physiol 2001;280:610–20.
[20] Myers JH, Stirling MC, Choy M, Buda AJ, Gallager KP. Direct measurement of inner and outer wall thickening dynamics with epicardial echocardiography. Circulation 1986;74:164–72.
[21] Sabbah HN, Marzilli M, Stain PD. The relative role of subendocardium and subepicardium in left ventricular mechanics. Am J Physiol Heart Circ Physiol 1981;240:920–7.
[22] Gallagher KP, Osakada G, Matuzaki M, Miller M, Kemper WS, Ross Jr J. Nonuniformity of inner and outer systolic wall thickening in conscious dogs. Am J Physiol Heart Circ Physiol 1985;249:241–8.
[23] Shapiro E, Marier DL, St John Sutton MG, Gibson DG. Regional non-uniformity of wall dynamics in normal left ventricle. Br Heart J 1981;45:264–70.
[24] Miyatake K, Yamagisi M, Tanaka N, Uematsu M, Yamazaki N, Mine Y, Sano A, Hirama M, Yamagishi M. New method for evaluation left ventricular wall motion by color-coded tissue Doppler imaging: in vitro and in vivo study. JACC 1995;25:717–24.
[25] Derumeaux G, Ovize M, Loufoua J, Pontier G, Andre-Fouet X, Gribier A. Assessment of nonuniformity of transmural myocardial velocity by color-coded tissue Doppler imaging, Characterization of normal, ischemic and stunned myocardium. Circulation 2000;101:1390–5.
[26] Marcos-Alberca P, Garcia-Fernandez MA, Ledesma MJ, Malpica N, Santos A, Moreno M, Bermejo J, Antoranz JC, Desco MD. Intramyocardial analysis of regional systolic and diastolic function in ischemic heart disease with Doppler tissue imaging; role of the different myocardial layers. J Am Soc Echocardiogr 2002;15:99–108.
[27] Sato Y, Maruyama A, Ichihashi K. Myocardial strain of the left ventricle in normal children. J Cardiol 2012;60:145–9.
[28] Nishimura K, Okayama H, Inoue K, Saito M, Yoshii T, Hiasa G, Sumimoto T, Inaba S, Ogimoto A, Funada J, Higaki J. Direct measurement of the radial strain in the inner-half layer of the ventricular wall in hypertensive patients. J Cardiol 2012;59:64–71.
[29] Suzuki K, Akashi Y, Mizukoshi K, Kou S, Takai M, Izumo M, Hayashi A, Ohtaki E, Nobuoka S, Miyake F. Relationship between left ventricular ejection fraction and mitral annular displacement derived by speckle tracking echocardiography in patients with different heart diseases. J Cardiol 2012;60:55–60.
[30] Tanaka M, Sakamoto T, Sugawara S, Katahira Y, Tabuchi H, Nakajima H, Kurokawa T, Kanai H, Hasagawa H, Ohtsuki S. A new concept of the contraction–extension property of the left ventricular myocardium. J Cardiol 2014;63:313–9.
[31] Kanai H, Tanaka M. Minute mechanical-excitation wave-front propagation in human myocardial tissue. Jpn J Appl Phys 2011;50, 07HAO1–7.
[32] Sengupta PP, Korinek J, Belohlavek M, Narula J, Vannan MA, Jahangir A, Khandheria BK. Left ventricular structure and function: basic science for cardiac imaging. J Am Coll Cardiol 2006;48:1988–2001.
[33] Saleh S, Liakopoulas OJ, Buckberg GD. The septal motor of biventricular function. Eur J Cardiothorac Surg 2006;295:S126–38.
[34] Buckberg G, Mahajan A, Saleh S, Hoffman JIE, Coghlan C. Structure and function relationship of the helical ventricular myocardial band. J Thorac Cardiovasc Surg 2008;136:578–89.
[35] Yin FCP. Ventricular wall stress. Circ Res 1981;49:829–42.
[36] Tanaka M, Sakamoto T, Sugawara S, Nakajima H, Katahira Y, Kameyama T, Kanai H, Ohtsuki S. Physiological basis and clinical significances of left ventricular suction studied using echo-dynamography. J Cardiol 2011;58: 232–44.
[37] Tanaka M, Sakamoto T, Sugawara S, Nakajima H, Kameyama T, Katahira Y, Ohtsuki S, Kanai H. Spiral systolic blood flow in the ascending aorta and aortic arch analyzed by echo-dynamography. J Cardiol 2010;56:97–110.